Aberrant fucosylation of extracellular vesicles remodels the vascular microenvironment and promotes chemoresistance in myelodysplastic syndromes and acute myeloid leukemia

Jingjing Feng,[1,2*] Kexin Wang,[1*] Junjie Gou,[1,3*] Yi Wang,[4] Bowen Hu,[1] Wei Wei,[1] Junqi Ge,[1] Yanli Feng,[4] Shuang Feng,[1] Eric Solary,[2] Feng Guan[1] and Xiang Li[1,5]

[1]Key Laboratory of Resource Biology and Biotechnology of Western China, Ministry of Education; Provincial Key Laboratory of Biotechnology, College of Life Sciences, Northwest University, Xi'an, China; [2]INSERM U1287, Université Paris-Saclay, Gustave Roussy Cancer Center, Villejuif, France; [3]Xi'an No. 1 Hospital, First Affiliated Hospital of Northwest University, School of Medicine, Xi'an, China; [4]Department of Hematology, Provincial People's Hospital, Xi'an, China and [5]Institute of Hematology, School of Medicine, Northwest University, Xi'an, China

**JF, KW and JGo contributed equally as first authors.*

Correspondence: X. Li
xiangli@nwu.edu.cn

Received: May 6, 2025.
Accepted: February 26, 2026.
Early view: March 5, 2026.

https://doi.org/10.3324/haematol.2025.288146

©2026 Ferrata Storti Foundation
Published under a CC BY-NC license

Aberrant fucosylation of extracellular vesicles remodels the vascular microenvironment and promotes chemoresistance in myelodysplastic syndromes and acute myeloid leukemia

Jingjing Feng[1,2#], Kexin Wang[1#], Junjie Gou[1,3#], Yi Wang[4], Bowen Hu[1], Wei Wei[1], Junqi Ge[1], Yanli Feng[4], Shuang Feng[1], Eric Solary[2], Feng Guan[1], Xiang Li[1,5*]

1. Key Laboratory of Resource Biology and Biotechnology of Western China, Ministry of Education; Provincial Key Laboratory of Biotechnology, College of Life Sciences, Northwest University, Xi'an, China.
2. INSERM U1287, Université Paris-Saclay, Gustave Roussy Cancer Center, Villejuif, France.
3. Xi'an No. 1 Hospital, First Affiliated Hospital of Northwest University, School of Medicine, Xi'an, China.
4. Department of Hematology, Provincial People's Hospital, Xi'an, China.
5. Institute of Hematology, School of Medicine, Northwest University, Xi'an, China.

The authors have declared that no conflict of interest exists.

# Authors contributed equally.

*Correspondence to Xiang Li (e-mail: xiangli@nwu.edu.cn), Tel: +86-29-88303534, College of Life Science, Northwest University, 229 Taibai North Road, Xi'an, Shaanxi 710069, China

Supplemental methods

Cell lines and cell culture

Human leukemia-derived cell line KG1a and DAC-resistant KG1a (KG1a-DAC)[1] were cultured in RPMI 1640 medium, human umbilical vein endothelial cell line HUVEC and embryonic kidney cell line HEK-293T were cultured in DMEM (Biological Industries; Kibbutz Beit Haemek, Israel). All medium was supplemented with 10% fetal bovine serum (FBS) (Biological Industries). All cells were maintained at 37°C in a 5% CO_2 atmosphere and routinely tested for Mycoplasma with the GMyc-PCR Mycoplasma Test Kit (#40601ES20, Yeasen, Shanghai, China).

Preparation of conditioned medium (CM) and sEVs

Cells were incubated in FBS-free medium for 48 h. The supernatant was collected and centrifuged at 500 × g for 10 min, and then filtered with 0.22 μm filter as CM.

To prepare sEVs, CM was sequentially centrifuged at 2000 × g for 20 min, 10,000×*g* for 30 min at 4 °C, and ultracentrifuged twice at 100,000 × g (Optima XE-100; Beckman Coulter Life Sciences; Indianapolis, IN, USA) for 70 min.[2] Pellets were resuspended in PBS and stored at -80 °C.

Characterization of sEVs

Isolated sEVs were placed on 400-mesh carbon-coated grids (Electron Microscopy Sciences; Fort Washington, PA, USA) and stained with 2% uranyl acetate. Images were captured using a transmission electron microscopy (TEM) (model H-7650; Hitachi; Tokyo). Nanoparticle tracking analysis (NTA) was performed using the Zetaview-PMX120-Z instrument (Particle Metrix, Meerbusch, Germany).

Permeability assay

HUVECs (6×10^4) were plated on 0.4 μm transwell filters in a 12-well plate (Jet Biofil), and treated with CM or sEVs (50 μg/mL) for 48 h. Rhodamine B (RB)-dextran (70 kDa; Sigma-Aldrich, St. Louis, MO, USA) was added to the upper well to a final concentration of 10 μg/mL. Following an incubation period of 30 minutes, the fluorescence intensity in the lower chamber was quantified using a microplate reader, with an excitation wavelength at 544 nm and an emission wavelength at 590 nm.

Transendothelial migration analysis

HUVECs (3×10^4) were plated on 8 μm transwell filters in a 12-well plate (Jet Biofil) to form a monolayer, and treated with CM or sEVs (50 μg/mL) for 48 h. Subsequently, 1×10^4 stable GFP-expressing KG1a cells were added into upper chamber and cultured for 24 h. Afterward, the cells migrated to the lower chamber were harvested, and the GFP fluorescence intensity of these cells was assessed using flow cytometry.

Tube formation assay

HUVECs were incubated with serum-free medium for 12 h, and then seeded at 2×10^4 cells per well in 96-well plates precoated with Matrigel matrix (Corning, NY, USA). These cells were treated with CM or sEVs (50 μg/mL) for 4–6 h. Tube formation was observed and documented photographically under a microscope.

SDS-PAGE and Western blotting

Cells were collected and lysed with RIPA buffer (50 mM Tris, pH 7.2, 1% Triton X-100, 0.5% sodium deoxycholate, 0.1% SDS, 150 mM NaCl, 10 mM $MgCl_2$ and 5% glycerol) containing 1% PMSF. Protein concentration was determined using BCA

Protein Assay Kit (#P0011, Beyotime, Nanjing, China). Proteins (25 μg) from each lysate were separated by electrophoresis in a 10% polyacrylamide resolving gel and transferred onto a polyvinylidene difluoride (PVDF) membranes. After blocking with 3% BSA (#ST023, Beyotime) in Tris-buffered saline containing 0.1% Tween-20 (TBST) at RT for 1 h, membranes were incubated at 4°C overnight in TBS-T containing following antibodies against Alix (#92880S, Cell Signaling Technology, MA, USA), Calnexin (#2679S), IκBα (#9242), p65 (#8242), p- IκBα (#2859), p- p65 (#3031), FUT4 (#19497-1-AP, proteintech, Wuhan, China), CD15 (#sc-19595), Occludin (#sc-133256), Claudin-5 (#sc-374221), ZO1 (#sc-33725, Santa Cruz Biotechnology, USA), TSG101 (#T55985, Abmart, Shanghai, China), followed by the addition of secondary antibody conjugated with HRP (#A0208, #A0216, Beyotime). Bands were visualized by enhanced chemiluminescence (ECL; Vazyme Biotech, Nanjing, China).

Detection of Le^X on sEVs by lectin-based ELISA

To determine the levels of Le^X on sEVs, 96-well ELISA plates were pre-coated with 100 μL/well of anti-CD63 antibody (sc-365604, Santa Cruz Biotechnology) and incubated for 12 h at 4 °C. The plates were washed three times with PBST (0.05% Tween-20 in PBS) and blocked with 1% BSA for 1 h at 37 °C. sEVs samples were added and incubated for 2 h at 37 °C. After washing with PBST, the wells were incubated with biotinylated Aleuria aurantia lectin for 2 h at 37 °C, followed by incubation with HRP-conjugated streptavidin for 30 min at 37 °C. The plates were developed using 3,3′,5,5′-tetramethylbenzidine (TMB) substrate (Promega, Madison, USA) and the reaction was stopped with 2 M H_2SO_4. Absorbance was measured at

450 nm using a microplate reader.

Proteomic analysis

Proteins (100 µg) were denatured with 8 M urea, reduced by 5 mM dithiothreitol (DTT) for 1 h at RT, alkylated with 20 mM iodoacetamide (IAM) for 30 min in the dark at RT, diluted with deionized water to lower urea concentration below 2 M, digested with lysyl endopeptidase (Wako Puro Chemical; Osaka, Japan) for 4 h at 37 °C, and digested with trypsin (Promega) overnight at 37 °C. The mixture was acidified with 10% trifluoroacetic acid (TFA) to pH< 3 and purified using C18 cartridges (Waters Corp.; Taunton, MA, USA). Two-dimensional liquid chromatography/ mass spectrometry (LC-MS) was performed on LTQ8 Orbitrap MS (Thermo Fisher; San Jose, CA, USA) and data were analyzed using Proteome Discoverer software (Thermo Fisher), with quantification by MaxQuant software program v2.6.7.0 (maxquant.org).[3]

N-glycan analysis

Glycomic analysis was performed as previously described.[4] A volume of 10 µL serum or 1 mg of sEVs was added onto a size-exclusion spin ultrafiltration unit (Millipore; Billerica, MA, USA). Proteins were denatured with 8 M urea/ 50 mM NH4HCO3, reduced with dithiothreitol (DTT), alkylated with iodoacetamide (IAM), and digested with PNGase F overnight at 37 °C. Released N-glycans were collected by centrifugation, lyophilized, and desalted using HyperSep Hypercarb solid phase extraction (SPE) cartridge (ThermoFisher Scientific; Waltham, Massachusetts, US).

Lyophilized N-glycans were dissolved and spotted onto an MTP AnchorChip sample target with 20 mg/mL 2,5-dihydroxybenzoic acid (DHB) as the matrix.

Measurements were taken in positive-ion mode. Each full-mass scan was performed with following conditions: acceleration voltage, 24.59 kV; reflector voltage, 26.6 kV; pulsed ion extraction, 100 ns; mass range, 1000–3500 m/z. For the data analysis, the peaks were smoothed and baseline subtraction performed three times. Relative intensity was analyzed and generated using FlexAnalysis software (Bruker Daltonics; Bremen, Germany) based on MALDI-TOF/TOF–MS intensity. m/z data were annotated using GlycoWorkbench software,[5] and cross-referenced with previous studies. [6-8]

Chromatin immunoprecipitation assay (ChIP)

The ChIP assay was performed as described previously.[9] Briefly, KG1a-TWIST1 cells[10] were cross-linked with 1% formaldehyde. Subsequently, DNA was fragmented to an average length of 200 to 500 bp using a sonicator (#Ymnl-1000Y, Nanjing, China). Immunoprecipitation was performed using antibody against TWIST1 (#ab50887, Abcam). Protein A/G agarose was added and rotated for 4 h. The samples were subsequently treated with proteinase K (#ST532, Beyotime) and RNase A (#ST578, Beyotime). Target DNA was extracted using phenol/chloroform and analyzed by PCR with the primers in Tab. S2.

Dual luciferase reporter assay

The wild type and mutant regions of FUT4 promoter were amplified by PCR and cloned into pGL3 vector (#E1751, Promega; Madison, WI, USA). Then the pGL3 vector containing the wild-type or mutant FUT4 promoter regions was co-transfected into HEK-293T cells along with the Renilla luciferase expression plasmid (pRL-TK, #D2760, Beyotime) and the TWIST1 overexpression plasmid. After 48 h, luciferase activity was

measured with a Dual Luciferase Reporter Assay System (#RG028, Beyotime). The primers for PCR have been shown in Tab.S3.

OptiPrep density gradient purification

sEVs were purified by OptiPrep density gradient as described previously.[11] In brief, 40%, 20%, 10%, and 5% (w/v) iodixanol solutions were prepared by diluting OptiPrep (60% (w/v) aqueous iodixanol, Axis-Shield PoC; AS; Oslo, Norway) with 0.25 M sucrose/ 10 mM Tris, pH 7.5 in 14 × 89 mm Ultra-Clear tubes. sEVs purified by ultracentrifugation were placed on top of the gradient, continuous gradient was established through ultracentrifugation at 100,000 × g for 18 h using a Beckman Coulter Optima XE-100 and Ti45 rotor, and twelve fractions were collected. Each fraction was diluted in PBS, pelleted through another round of ultracentrifugation at 100,000 x g for 3 h, and washed with and resuspended in PBS.

Supplementary figures with legends.

Fig. S1. (A) Permeability of HUVEC monolayers to rhodamine B–labeled dextran (RB-dextran) after coculture with KG1a or KG1a-DAC for 48 h. (B) Immunoblot analysis of tight junction proteins in HUVECs cocultured with KG1a or KG1a-DAC. (C) Representative images of tube formation. (D) Immunoblot analysis of tight junction–related proteins in HUVECs treated with conditioned medium (CM) from KG1a or KG1a-DAC. (E) RB-dextran permeability and (F) transendothelial migration after CM treatment. (G) Quantification of junction count and total branching length in HUVECs treated with CM. Data are mean ± SEM; experiments were repeated three times with similar results. **P<0.01; ***P<0.001.

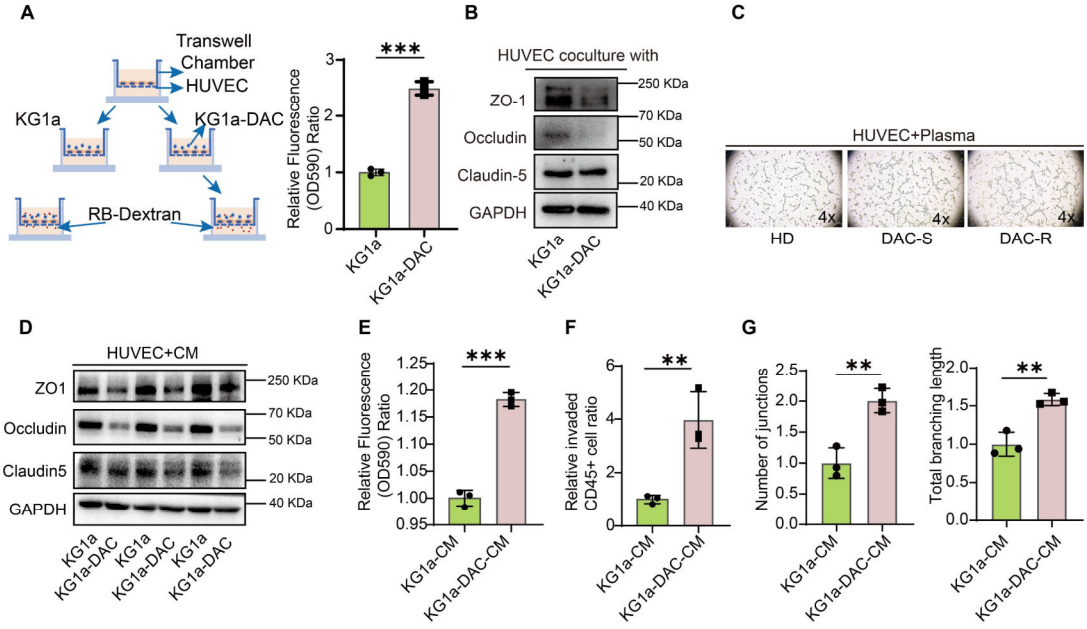

Fig. S2. (A-F) Characteristic of small extracellular vesicles (sEVs) using TEM (A&B), NTA (C&D), and western blotting (E&F). (G)Tube formation assay.

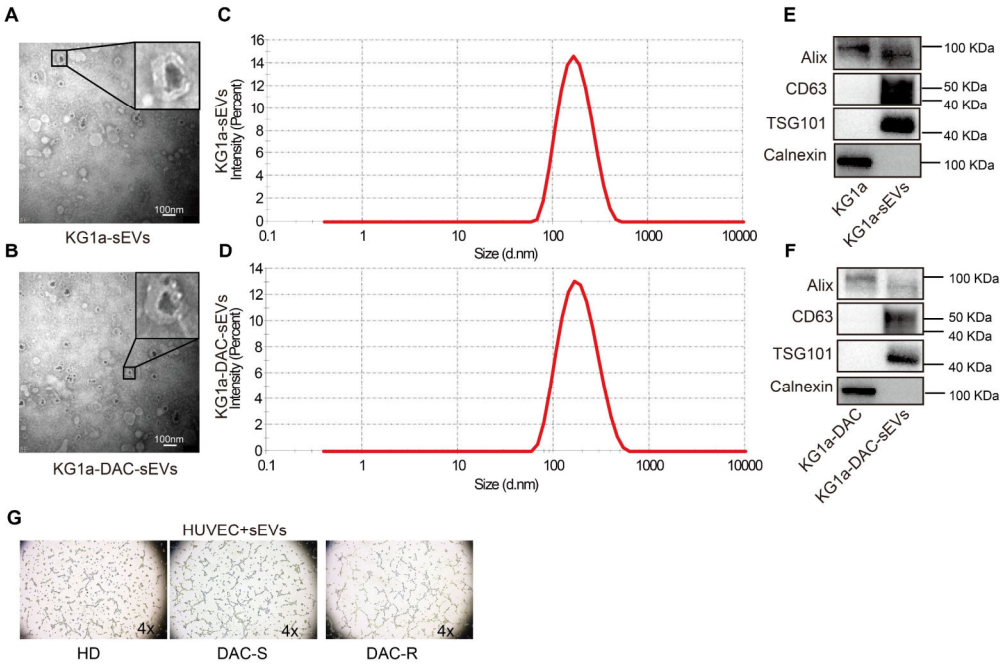

Fig. S3. (A-C) MALDI-TOF/TOF–MS spectra of N-glycans in myelodysplastic syndromes/acute myeloid leukemia (MDS/AML) patients who are sensitive to DAC treatment (DAC-S) or are refractory to DAC treatment (DAC-R) serum samples. Peaks

of MALDI-TOF/TOF–MS spectra (signal-to-noise ratio>5) were selected for relative intensity analysis. Glycan compositions are annotated using the H/N/F/S nomenclature (H, hexose; N, N-acetylglucosamine; F, fucose; S, sialic acid).

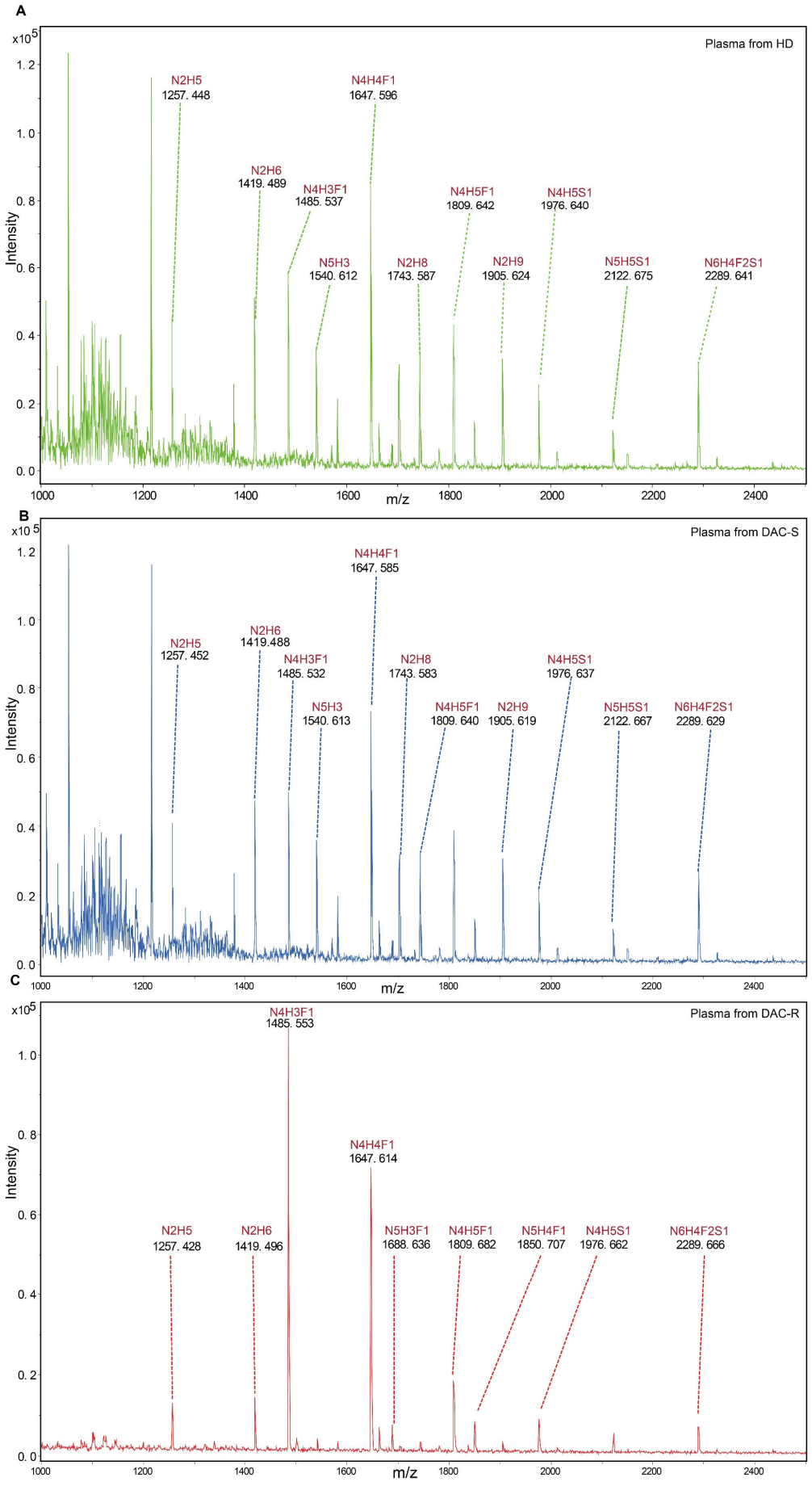
A
Plasma from HD
x10 5
Intensity
m/z
N2H5 1257. 448
N4H4F1 1647. 596
N2H6 1419. 489
N4H3F1 1485. 537
N4H5F1 1809. 642
N4H5S1 1976. 640
N5H3 1540. 612
N2H8 1743. 587
N2H9 1905. 624
N5H5S1 2122. 675
N6H4F2S1 2289. 641
B
Plasma from DAC-S
N4H4F1 1647. 585
N2H5 1257. 452
N2H6 1419.488
N4H3F1 1485. 532
N2H8 1743. 583
N4H5S1 1976. 637
N5H3 1540. 613
N4H5F1 1809. 640
N2H9 1905. 619
N5H5S1 2122. 667
N6H4F2S1 2289. 629
C
Plasma from DAC-R
N4H3F1 1485. 553
N4H4F1 1647. 614
N2H5 1257. 428
N2H6 1419. 496
N5H3F1 1688. 636
N4H5F1 1809. 682
N5H4F1 1850. 707
N4H5S1 1976. 662
N6H4F2S1 2289. 666

Fig. S4. (A) Relative abundance of fucosylated and non-fucosylated N-glycans in plasma from healthy donors (HD), decitabine-sensitive (DAC-S), and decitabine-refractory (DAC-R) patients. (B) Relative intensity of individual fucosylated N-glycan compositions in plasma from HD, DAC-S, and DAC-R patients. (C) Fold change of individual fucosylated N-glycan compositions normalized to the HD group. (D) Representative MALDI-TOF/TOF–MS spectra of N-glycans in sEVs from KG1a and KG1a-DAC cells. Peaks with signal-to-noise ratio >5 were included for relative intensity analysis. Glycan compositions are annotated using the H/N/F/S nomenclature (H, hexose; N, N-acetylglucosamine; F, fucose; S, sialic acid). (E) Relative intensity of individual N-glycan compositions in sEVs from KG1a and KG1a-DAC cells. (F) AAL-reactive signal in plasma from HD, DAC-S, and DAC-R samples determined by ELISA. (G) Immunoblot analysis of FUT4 expression in KG1a and KG1a-DAC cells. (H) Le^X levels in KG1a-DAC cells with or without PNGase F treatment. (I) Le^X levels in plasma-derived sEVs from HD, DAC-S, and DAC-R samples. (J) Le^X levels in KG1a and KG1a-DAC cells assessed by flow cytometry (representative histograms and mean fluorescence intensity quantification). Data are mean ± SEM; experiments were repeated three times with similar results. ns, not significant; *P<0.05; **P<0.01; ***P<0.001.

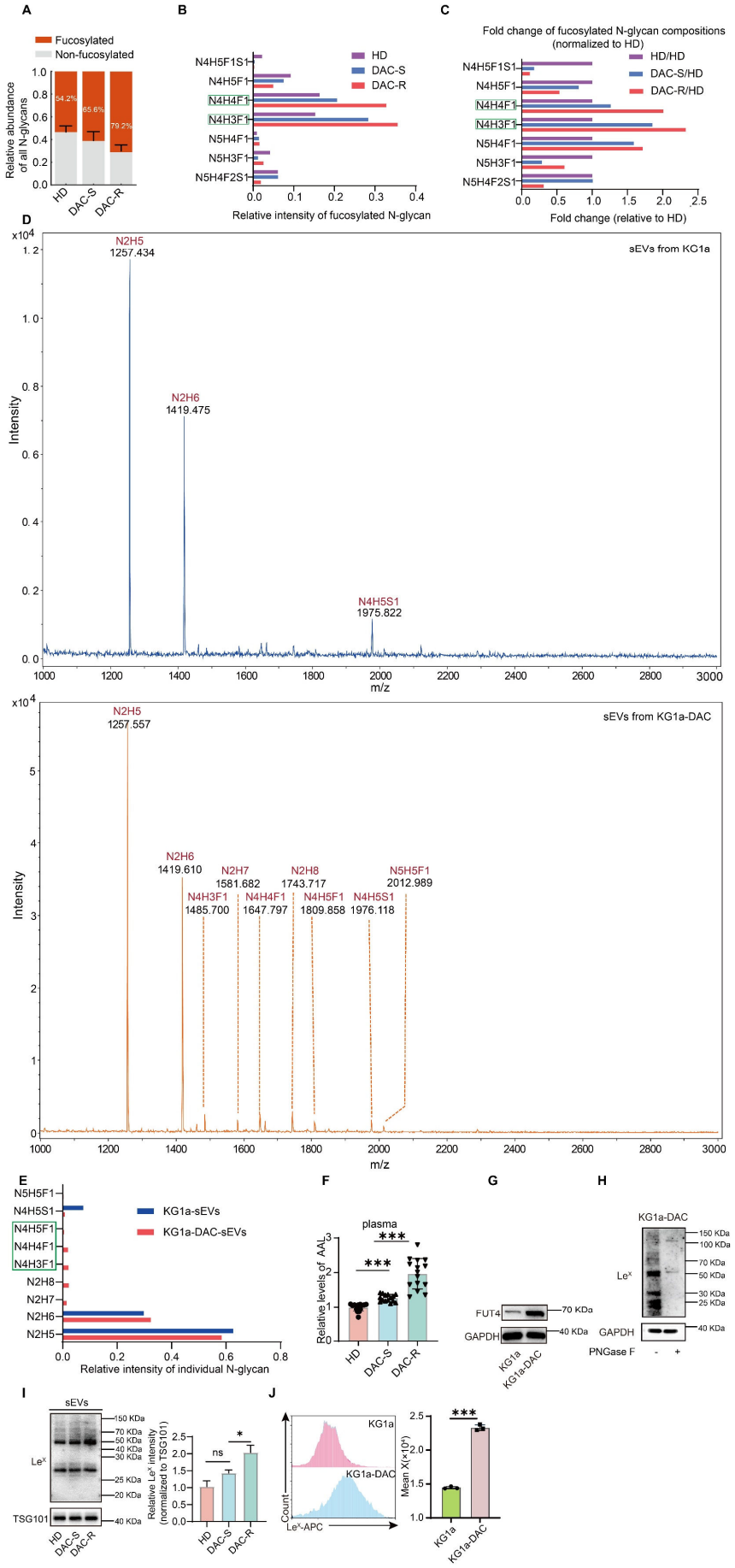
A
Fucosylated
Non-fucosylated
Relative abundance of all N-glycans
54.2%
65.6%
79.2%
HD
DAC-S
DAC-R
B
HD
DAC-S
DAC-R
N4H5F1S1
N4H5F1
N4H4F1
N4H3F1
N5H4F1
N5H3F1
N5H4F2S1
Relative intensity of fucosylated N-glycan
C
Fold change of fucosylated N-glycan compositions (normalized to HD)
HD/HD
DAC-S/HD
DAC-R/HD
Fold change (relative to HD)
D
sEVs from KG1a
N2H5
1257.434
N2H6
1419.475
N4H5S1
1975.822
Intensity
m/z
sEVs from KG1a-DAC
N2H5
1257.557
N2H6
1419.610
N2H7
1581.682
N2H8
1743.717
N5H5F1
2012.989
N4H3F1
1485.700
N4H4F1
1647.797
N4H5F1
1809.858
N4H5S1
1976.118
E
KG1a-sEVs
KG1a-DAC-sEVs
Relative intensity of individual N-glycan
F
plasma
Relative levels of AAL
HD
DAC-S
DAC-R
G
FUT4
70 KDa
GAPDH
40 KDa
KG1a
KG1a-DAC
H
KG1a-DAC
Le^x
GAPDH
PNGase F
I
sEVs
Le^x
TSG101
HD
DAC-S
DAC-R
Relative Le^x intensity (normalized to TSG101)
ns
J
KG1a
KG1a-DAC
Count
Le^x-APC
Mean X(×10^4)

Fig. S5. (A) Immunoblot analysis of tight junction–related proteins in human umbilical vein endothelial cells (HUVECs) after exposure to conditioned medium (CM) from KG1a or KG1a-FUT4. (B, C) HUVEC permeability to rhodamine B–labeled dextran (OD590) and transendothelial migration (relative invaded $CD45^+$ cell ratio) after exposure to the indicated CM. (D) Angiogenesis metrics (junction count and total branching length) in HUVECs treated with the indicated CM. (E, F) FUT4 expression and Lewis X (Le^X) levels in KG1a-DAC-shFUT4 cells and their derived small extracellular vesicles (sEVs). (G, H) Immunoblot analysis of tight junction–related proteins in HUVECs after exposure to CM or sEVs from KG1a-DAC or KG1a-DAC-shFUT4. (I, J) HUVEC permeability (OD590) and transendothelial migration (relative invaded $CD45^+$ cell ratio) after exposure to the indicated sEVs or CM. (K, L) Angiogenesis metrics (junction count and total branching length) in HUVECs treated with the indicated CM or sEVs. (M) Immunoblot analysis of tight junction–related proteins in HUVECs treated with OptiPrep-purified sEVs from KG1a, KG1a-DAC, KG1a-FUT4, and KG1a-DAC-shFUT4 cells. (N) Quantification of human $CD45^+$ cells in blood, bone marrow, and spleen in mice preconditioned with HD-sEVs or KG1a-sEVs. Data are mean ± SEM; experiments were repeated three times with similar results. *P<0.05; **P<0.01; ***P<0.001.

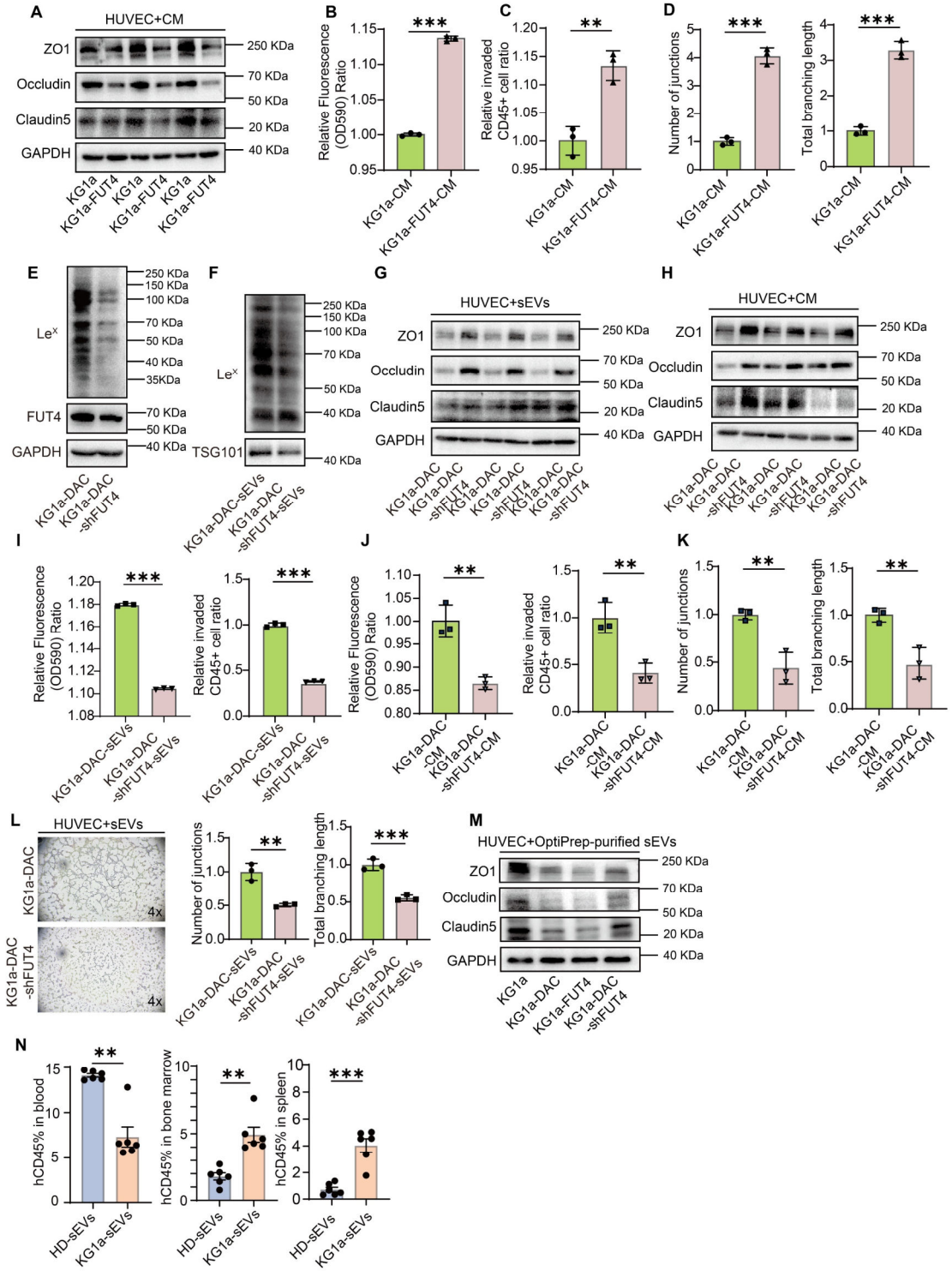

Fig. S6. (A) Expression of FUT4 and TWIST1 at mRNA levels in KG1a and KG1a-TWIST1 cells. (B&C) Expression of FUT4, TWIST1 at protein and mRNA levels and the levels of Le^X in SKM1 and SKM1-shTWIST1 cells. (D) Tight junction related-proteins and (E&F) permeability in HUVECs after treated with CM from SKM1 and

SKM1-shTWIST1. (G) Angiogenesis metrics in HUVECs treated with CM from SKM1 and SKM1-shTWIST1. (H) TWIST1 binding to E-box motifs within the 0–2000 bp region of the FUT4 promoter. (I) TWIST1 binding sites on wild-type (WT) and mutant sequences of E-box motif 1, 2 and 7 of FUT4 promoter. Data are mean ± SEM; experiments were repeated three times with similar results. *P<0.05; **P<0.01; ***P<0.001.

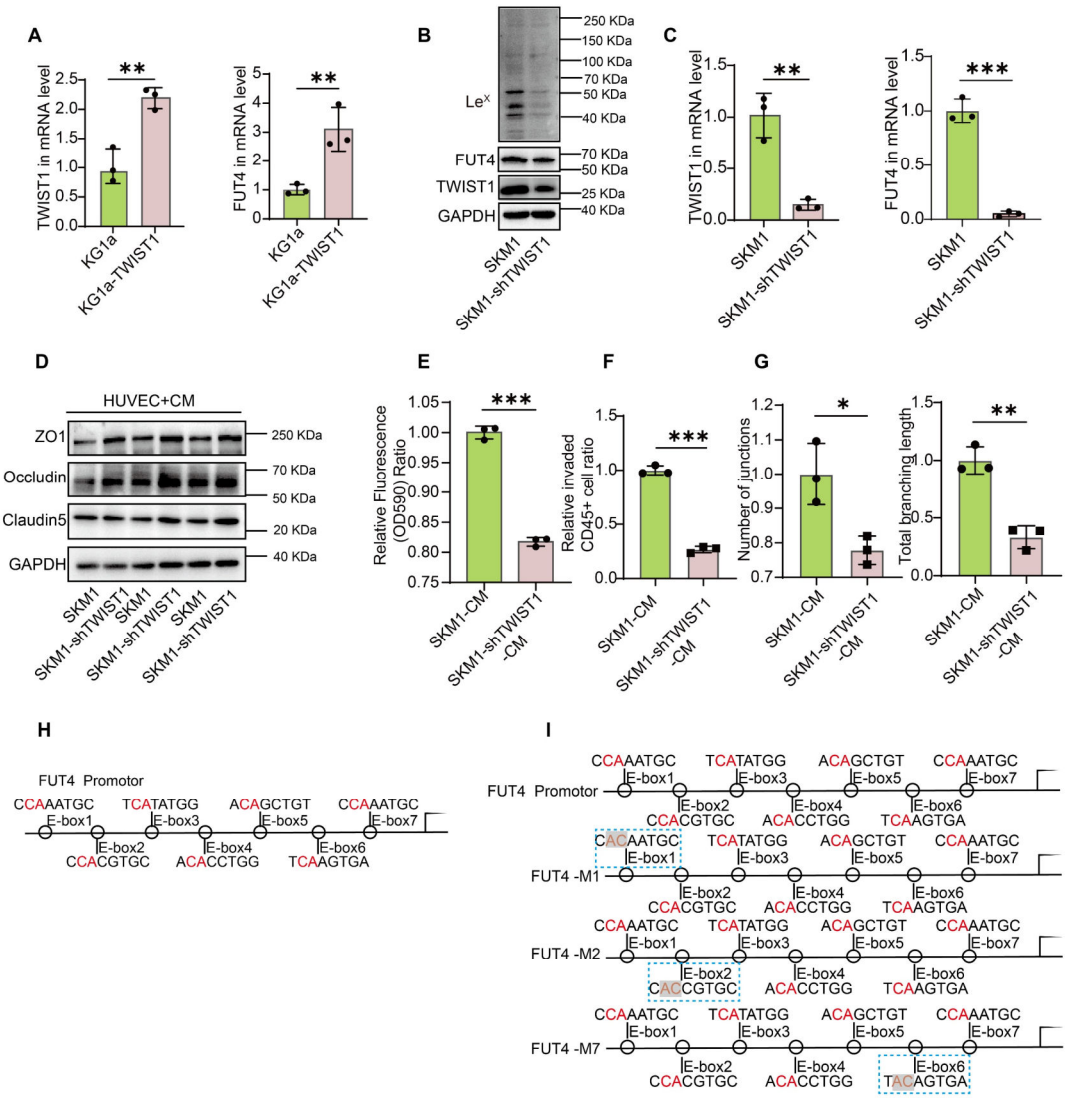

Fig. S7. (A) Immunoblot analysis of density gradient fractions showing sEV markers and ICAM3 in sEVs isolated from KG1a cells. (B) Expression of ICAM3 and Le^X in OptiPrep-purified sEVs derived from KG1a, KG1a-DAC, KG1a-FUT4, and KG1a-DAC-

shFUT4 cells. (C) Expression of ICAM3 in ultracentrifugation-isolated sEVs from the indicated cells. (D) ICAM3 stability in KG1a and KG1a-FUT4 cells after cycloheximide (CHX) treatment for the indicated times. (E) ICAM3 expression in KG1a cells treated with CHX in the presence or absence of MG132 or chloroquine (Chlo) for 8 h. (F–J) Immunoblot analysis of NF-κB signaling components (p65, p-p65, IκBα, p-IκBα) and tight junction–related proteins in HUVECs treated with BAY-11-7082 (F, G), phorbol 12-myristate 13-acetate (PMA) (H, I), or sEVs from the indicated cells (J).

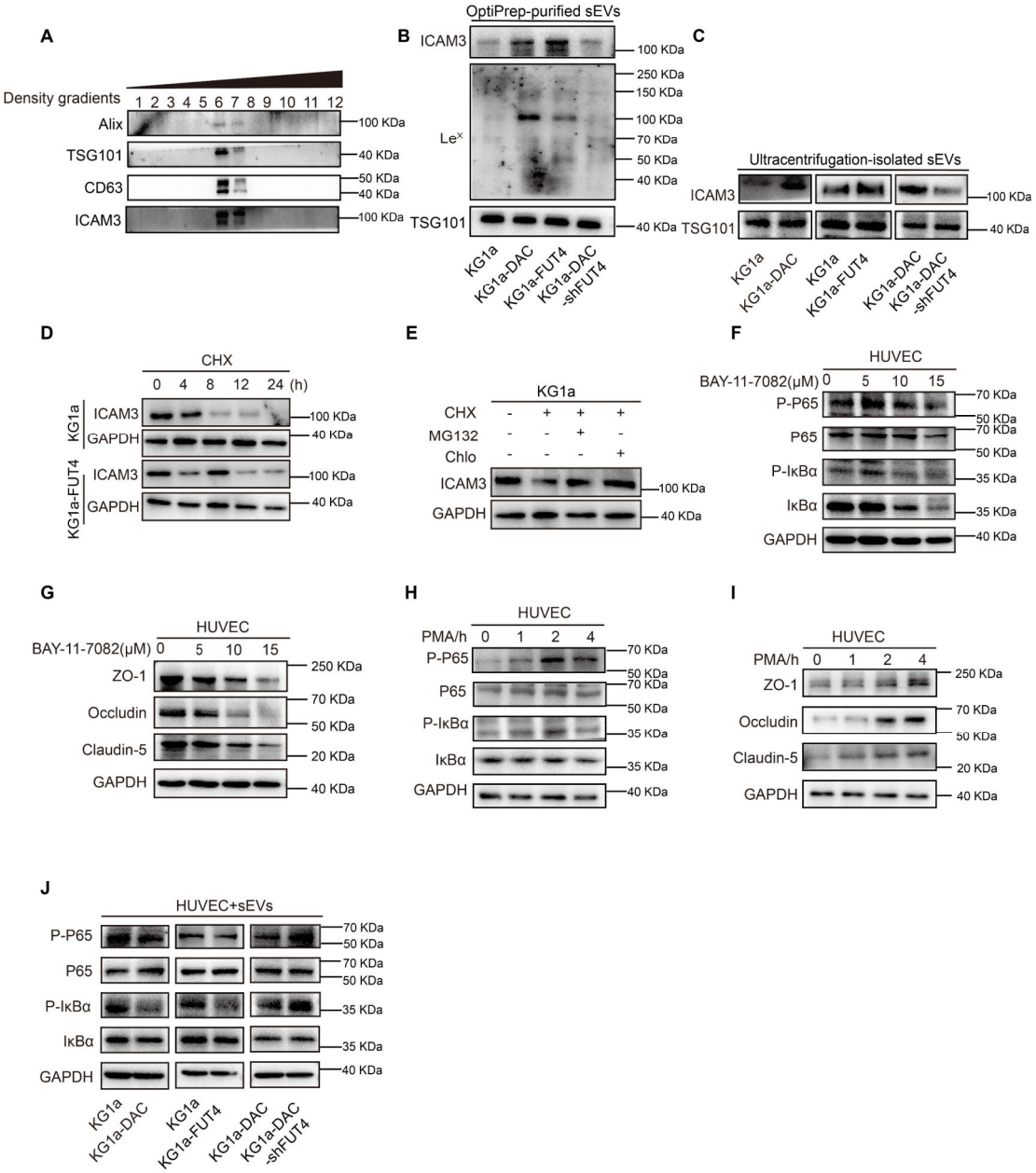

Fig. S8. (A) Expression of tight junction–related proteins and NF-κB signaling components (p65, p-p65, IκBα, p-IκBα) in HUVECs cocultured with KG1a-DAC cells in the presence or absence of anti-human ICAM3 antibody (a-ICAM3). (B, C) HUVEC permeability and leukemic cell transendothelial migration, and (D) angiogenesis metrics of HUVECs cocultured with indicated cells with or without a-ICAM3. (E) Expression of tight junction–related proteins and NF-κB signaling components (p65, p-p65, IκBα, p-IκBα) in HUVECs cocultured with KG1a-DAC-shFUT4 cells with or without

recombinant ICAM3 (rICAM3). (F, G) HUVEC permeability and leukemic cell transendothelial migration, and (H) angiogenesis metrics of HUVECs cocultured with indicated cells with or without rICAM3. (I) Immunoblot analysis of ICAM3 and NF-κB signaling components (p65, p-p65, IκBα, p-IκBα) in HUVEC and HUVEC-ICAM3. (J) Immunoblot analysis of tight junction–related proteins and ICAM3 in HUVEC and HUVEC-ICAM3. (K, L) HUVEC permeability and leukemic cell transendothelial migration in HUVEC and HUVEC-ICAM3. (M) Angiogenesis metrics, including junction count and total branching length, were quantified in HUVEC and HUVEC-ICAM3. Data are mean ± SEM; experiments were repeated three times with similar results. *P<0.05; **P<0.01; ***P<0.001.

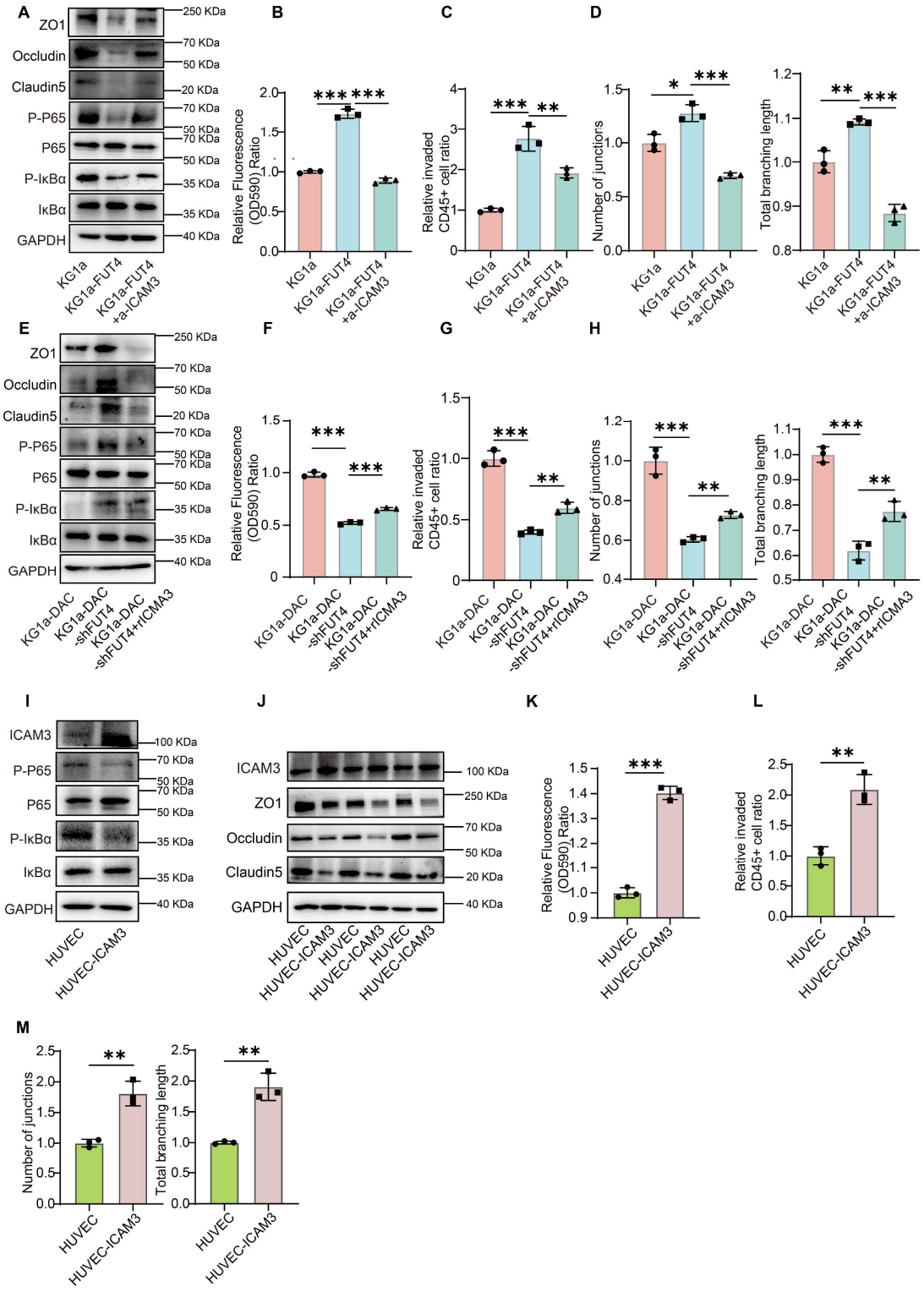

Supplementary tables

Tab. S1 Patients list

Diagnosis	Age	Gender	Cytogenetics	BM Cellularity	Marrow Blast Count	DAC Response

AML	69	M	Normal	Hypercellular	41%	R
MDS-EB2	54	M	Normal	Normal	16.80%	R
AML	73	F	Normal	Hypercellular	43%	R
AML	48	M	Normal	Hypercellular	45%	R
AML	31	F	Normal	Hypercellular	53%	R
AML	48	F	Normal	Hypercellular	61%	R
MDS-EB1	35	M	Normal	Hypercellular	12%	R
MDS-EB2	31	M	Normal	Hypercellular	14%	R
MDS-EB2	56	M	Normal	Hypercellular	13%	R
AML	77	F	Normal	Hypercellular	24%	R
AML	64	M	Normal	Normal	35%	R
MDS-EB2	72	F	Normal	Normal	17%	R
AML	53	F	Normal	Hypercellular	27%	R
AML	62	F	t(8;21)(q22;q22)	Normal	30%	R
MDS-EB2	65	M	Normal	Hypercellular	15%	R
MDS-EB1	75	F	Normal	Hypercellular	12%	R
MDS-EB2	76	F	Normal	Hypercellular	14%	R
AML	67	F	Normal	Hypercellular	25%	R
AML	70	M	Normal	Hypercellular	25%	R
AML	78	F	Normal	Normal	40%	S
MDS-MLD	65	M	Normal	Normal	6.50%	S
MDS-EB1	62	M	Normal	Normal	8%	S
AML	48	M	t(8;21)(q22;q22)	Hypercellular	23.50%	S
AML	58	M	Normal	Hypercellular	29%	S
MDS-EB2	66	F	Complex karyotype	Normal	23%	S
AML	43	F	t(8;21)(q22;q22), +8	Hypercellular	29%	S
AML	58	F	Normal	Normal	32%	S
AML	68	M	Normal	Normal	22%	S
MDS-EB1	44	F	Normal	Normal	5%	S
MDS-EB1	61	F	Normal	Hypercellular	9%	S
MDS-EB2	75	F	Complex karyotype	Hypercellular	14%	S
AML	30	M	Normal	Hypercellular	30%	S
AML	79	M	Normal	Normal	45%	S
AML	32	F	t(8;21)(q22;q22)	Hypercellular	36%	S
AML	68	F	Normal	Hypercellular	28%	S
MDS-EB2	76	M	Complex karyotype	Normal	25%	S

MDS-EB1	74	M	Normal	Normal	8%	S
HD	45	F				
HD	36	F				
HD	35	M				
HD	58	F				
HD	27	M				
HD	36	F				
HD	45	F				
HD	28	F				
HD	61	F				
HD	23	F				
HD	57	M				
HD	60	M				
HD	61	M				
HD	49	M				
HD	28	M				
HD	70	F				
HD	61	F				
HD	69	M				
HD	48	M				

Tab. S2 Primer list for chip

Primers	Sequences
FUT4-E-box-1-F	CGAGGTAAGAGGGCACAAAGAAAAT
FUT4-E-box-1-R	AGGCATTTGGGAAATATTACCCTGC
FUT4-E-box-2-F	GCCACGTGCCAGACACAATGTT
FUT4-E-box-2-R	AGGTGTTCTGGCTAGGCCCAT
FUT4-E-box-3-F	TCTCGATCTCCTGACCT
FUT4-E-box-3-R	ATTTGCGTTAGCCATATG
FUT4-E-box-4-F	AACACCTGGCAGGATTG
FUT4-E-box-4-R	AGCTGTGCATCAGTGGA
FUT4-E-box-5-F	AGTATCAGTGGGACTCCACT

FUT4-E-box-5-R	TCTGGGTGTTCGCTTTG
FUT4-E-box-6-F	TCTCAAGTGACTGTAGACGT
FUT4-E-box-6-R	ATTCTAGCACCCAAGTTAAGG
FUT4-E-box-7-F	GTTCTCTATCCTTTACTGGGCT
FUT4-E-box-7-R	AGACGGTCGAATTGTGGAG

Tab. S3 Primer list for dual luciferase reporter assay

Primers	Sequences
FUT4-F	AGATCGCCGTGTAATTCTAGATGCGAAGTCACGACTGGTTTC
FUT4-R	AGGGCATCGGTCGACGGATCCGGAGGATAGCGTCGGCTTCC
FUT4-E-BOX-1F'	GTAATATTTCCACAATGCCTACCGGCCACGT
FUT4-E-BOX-1R'	CGGTAGGCATTGTGGAAATATTACCCTGCTTGATTGC
FUT4-E-BOX-2F'	TACCGGCACCGTGCCAGACACAAT
FUT4-E-BOX-2R'	ATTGTGTCTGGCACGGTGCCGGTAGGCATTTGGGA
FUT4-E-BOX-7F'	CACACAATGCAGAGACTCTGAAGGCCA
FUT4-E-BOX-7R'	CCTTCAGAGTCTCTGCATTGTGTGAAGAACTTAAG

Tab. S4 see Excel File

Identified N-glycans in plasma from HD, DAC-S, and DAC-R patients and in sEVs from KG1a and KG1a-DAC cells, as determined by MALDI-TOF/TOF-MS.

Supplemental Reference

1. Lei L, Wang Y, Liu R, et al. Transfer of miR-4755-5p through extracellular vesicles and particles induces decitabine resistance in recipient cells by targeting CDKN2B. Mol Carcinog. 2023;62(6):743-753.

2. Sung BH, Ketova T, Hoshino D, Zijlstra A, Weaver AM. Directional cell movement through tissues is controlled by exosome secretion. Nat Commun. 2015;6:7164.

3. Beer LA, Liu P, Ky B, Barnhart KT, Speicher DW. Efficient Quantitative Comparisons of Plasma Proteomes Using Label-Free Analysis with MaxQuant. Methods Mol Biol. 2017;1619:339-352.

4. Cao L, Zhou Y, Li X, Lin S, Tan Z, Guan F. Integrating transcriptomics, proteomics, glycomics and glycoproteomics to characterize paclitaxel resistance in breast cancer cells. J Proteomics. 2021;243:104266.

5. Ceroni A, Maass K, Geyer H, Geyer R, Dell A, Haslam SM. GlycoWorkbench: a tool for the computer-assisted annotation of mass spectra of glycans. J Proteome Res. 2008;7(4):1650-1659.

6. Wang R, Liu Y, Wang C, et al. Comparison of the methods for profiling N-glycans-hepatocellular carcinoma serum glycomics study. RSC Adv. 2018;8(46):26116-26123.

7. Ramachandran P, Xu G, Huang HH, et al. Serum Glycoprotein Markers in Nonalcoholic Steatohepatitis and Hepatocellular Carcinoma. J Proteome Res. 2022;21(4):1083-1094.

8. Tsai TH, Wang M, Di Poto C, et al. LC-MS profiling of N-Glycans derived from human serum samples for biomarker discovery in hepatocellular carcinoma. J Proteome Res. 2014;13(11):4859-4868.

9. Li H, Wang Y, Feng S, et al. Reciprocal regulation of TWIST1 and OGT determines the decitabine efficacy in MDS/AML. Cell Commun Signal. 2023;21(1):255.

10. Li H, Wang Y, Pang X, et al. Elevated TWIST1 expression in myelodysplastic syndromes/acute myeloid leukemia reduces efficacy of hypomethylating therapy with decitabine. Haematologica. 2020;105(10):e502.

11. Tan Z, Cao L, Wu Y, et al. Bisecting GlcNAc modification diminishes the pro-metastatic functions of small extracellular vesicles from breast cancer cells. J Extracell Vesicles. 2020;10(1):e12005.